Polyhedron 29 (2010) 204–211

Contents lists available at ScienceDirect

Polyhedron

journal homepage: www.elsevier.com/locate/poly

Strong antiferromagnetic coupling in doubly *N*,*O* oximato-bridged dinuclear copper(II) complexes

Evangelia S. Koumousi [a], Catherine P. Raptopoulou [b], Spyros P. Perlepes [a], Albert Escuer [c], Theocharis C. Stamatatos [a,*]

[a] *Department of Chemistry, University of Patras, GR-265 04 Patras, Greece*
[b] *Institute of Materials Science, NCSR "Demokritos", GR-153 10 Aghia Paraskevi Attikis, Athens, Greece*
[c] *Departament de Quimica Inorganica, Universitat de Barcelona, Diagonal 647, 08028 Barcelona, Spain*

ARTICLE INFO

Article history:
Available online 5 August 2009

Keywords:
β-Diketonato ligands
Crystal structures
Di-2-pyridyl ketone oxime
Dinuclear copper(II) complexes
Magnetochemistry
Phenyl 2-pyridyl ketone oxime

ABSTRACT

The use of di-2-pyridyl ketone oxime, (py)pkoH, and phenyl 2-pyridyl ketone oxime, ppkoH, in copper(II) hexafluoroacetylacetonate chemistry is reported. The reaction of $CuCl_2{\cdot}2H_2O$ with one and two equivalents of ppkoH and Na(hfac), respectively, in CH_2Cl_2 affords the dinuclear complex $[Cu_2(hfac)_2(ppko)_2]$ (**1**) in excellent yield. The replacement of ppkoH by (py)pkoH gives the isostructural compound $[Cu_2(hfac)_2\{(py)pko\}_2]$ (**2**) in good yield. The Cu^{II} atoms in both **1** and **2** are doubly bridged by the oximate groups of two $\eta^1{:}\eta^1{:}\eta^1{:}\mu_2$ $ppko^-$ and $(py)pko^-$ ligands, respectively. The bridging Cu–(R–NO)–Cu′ units are not planar, with the torsion angles being 23.2° (**1**) and 20.3° (**2**). A bidentate chelating $hfac^-$ ligand completes five-coordination at each square pyramidal metal ion. The $hfac^-$-free reaction system $CuCl_2{\cdot}2H_2O$/(py)pkoH/NEt_3 (1:2:1) gives instead the mononuclear complex $[CuCl\{(py)pko\}\{(py)pkoH\}]$ (**3**) in very good yield. The Cu^{II} atom is coordinated by two *N*,*N*′-bidentate $(py)pko^-$/(py)pkoH chelates and a monodentate chloride anion resulting in a distorted square pyramidal geometry around the metal center. Variable-temperature, solid-state dc magnetic studies were carried out on the representative dinuclear complex **1** in the 2.0–300 K range. The data indicate a very strong antiferromagnetic exchange interaction and a resulting $S = 0$ ground state, which is well isolated from the $S = 1$ excited state. The J value of $-720\ cm^{-1}$ was derived from the fitting of the experimental data using the Hamiltonian $H = -J(S_1 \cdot S_2)$.

1. Introduction

There is currently a renewed interest in the coordination chemistry of oximes [1]. The research efforts are driven by a number of considerations. These include the employment of oximate ligands in the synthesis of homometallic [1,2] and heterometallic [1,2c,3] polynuclear complexes (clusters) and coordination polymers [4] with interesting magnetic properties, including single-molecule magnetism [2b–d,5] and single-chain magnetism [4,6] behaviors. Ligands containing one oxime group and one pyridyl group, without other donor atoms, are popular in coordination chemistry. Most of these ligands contain a 2-pyridyl group and thus are named 2-pyridyl oximes, (py)C(R)NOH (Scheme 1). The anionic forms, $(py)C(R)NO^-$, of these molecules are versatile ligands for a variety of research objectives, including μ_2 and μ_3 behavior [1a,2c]. Di-2-pyridyl ketone oxime [(py)pkoH, Scheme 1] occupies a special position amongst the 2-pyridyl oximes because the R group is also a 2-pyridyl group; the compound is thus a bis(2-pyridyl) oxime.

We have been exploring "ligand blend" reactions involving mainly carboxylates *and* the anions of 2-pyridyl oximes (Scheme 1) as a means to high-nuclearity 3d-metal species [2c,7,8–12]. Our results with Cr [7b,7c], Mn [7a,8], Fe [9], Co [10], Ni [11] and Cu [12] have been very encouraging. For example, the use of methyl 2-pyridyl ketone oxime (Scheme 1, R = Me) in Mn carboxylate chemistry has yielded a new family of triangular $\{Mn^{III}{}_3(\mu_3\text{-}O)\}^{7+}$ core-containing products; the products are very unusual in being ferromagnetically coupled with a resultant $S = 6$ ground-state spin and are the first triangular single-molecule magnets [8e,8f]. Furthermore, the reactions of various Cu^{II} carboxylate sources with (py)pkoH have provided access to the family of triangular complexes $[Cu_3(OH)(O_2CR)_2\{(py)pko\}_3]$ (R = various) containing the $\{Cu_3(\mu_3\text{-}OH)\}^{5+}$ core and possessing the extremely rare inverse 9-MC-3 motif [12a]. Other structurally characterized compounds derived from the general Cu^{II}/(py)pkoH reaction system are the dinuclear complex $[Cu_2\{(py)pko\}_4]$ [13a], the fascinating 18-MC-6 cluster $[Cu_6(ClO_4)\{(py)pko\}_6(MeCN)_6][Cu_6(ClO_4)_3\{(py)pko\}_6(MeCN)_4](ClO_4)_8$ [13b,13c], compounds [Cu3(OH)Cl-

---

[*] Corresponding author. Tel.: +30 2610 996020; fax: +30 2610 997118.
E-mail address: thstama@chemistry.upatras.gr (T.C. Stamatatos).

0277-5387/$ - see front matter © 2009 Elsevier Ltd. All rights reserved.
doi:10.1016/j.poly.2009.07.010

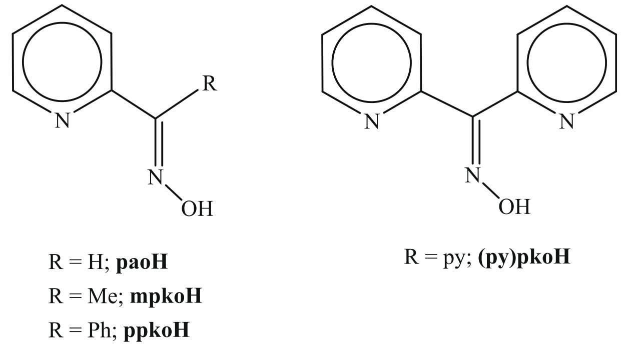

Scheme 1. General structural formulae and abbreviations of the 2-pyridyl oximes [(py)C(R)NOH] that are used in our laboratories, including phenyl 2-pyridyl ketone oxime (ppkoH) and di-2-pyridyl ketone oxime [(py)pkoH] employed in this work.

$\{(py)pko\}_3]_2(Ph_4B)_2$ and $[Cu_5\{(py)pko\}_7](ClO_4)_3$ [13c], the unique complex $[Cu_2Cl_4\{(py)pkoH_2\}_2(H_2O)_2]Cl_2$ that contains the monocation of (py)pkoH as ligand [13d], and the Cu^I complexes $[Cu(NCS)\{(py)pkoH\}]_n$ and $[Cu_2Cl_2\{(py)pkoH\}_2]$ [13e].

Since the RCO_2^- ions are structure-determining components in the $[Cu_3(OH)(O_2CR)_2\{(py)pko\}_3]$ complexes [12a], we anticipated that the absence of RCO_2^- from the reactions would give distinctly different new products, and we have therefore explored this possibility. We have investigated the reactions between the 2-pyridyl oximes ppkoH and (py)pkoH and a Cu^{II} β-diketonate starting material, namely copper(II) hexafluoroacetylacetonate ($hfac^-$). Note that β-diketonate ligands have been found to exhibit a dual role in the 3d-metal/organic ligand(s) chemistry: first, they can enhance the deprotonation of neutral organic ligands that bear ionizable hydrogen(s) acting as bases, and second they are excellent ancillary chelating/bridging groups favoring the formation of thermodynamically stable products. We herein report that the $Cu^{II}/hfac^-$/ppkoH and $Cu^{II}/hfac^-$/(py)pkoH reaction schemes have successfully led to two dinuclear, doubly *N,O* oximate-bridged complexes and to one interesting mononuclear, $hfac^-$-free compound which incorporates both the neutral and anionic forms of (py)pkoH. The syntheses, structures and magnetochemical characterization (for one representative Cu_2 complex) of these compounds are described in this paper.

2. Experimental

2.1. General and physical measurements

All manipulations were performed under aerobic conditions using materials (reagent grade) and solvents as received.

Microanalyses (C, H, N) were performed by the University of Ioannina (Greece) Microanalytical Laboratory using an EA 1108 Carlo Erba analyzer. IR spectra (4000–450 cm^{-1}) were recorded on Perkin–Elmer 16 PC FT spectrometer with samples prepared as KBr pellets. Variable-temperature magnetic studies for complex **1** were performed using a Quantum Design SQUID magnetometer at the Magnetochemistry Service of the University of Barcelona. Diamagnetic corrections were applied to the observed paramagnetic susceptibilities using Pascal's constants.

2.2. Compound preparation

2.2.1. $[Cu_2(hfac)_2(ppko)_2]$ (**1**)

To a stirred, colorless solution of ppkoH (0.20 g, 1.00 mmol) and Na(hfac) (0.46 g, 2.00 mmol) in CH_2Cl_2 (30 mL) was added solid $CuCl_2{\cdot}2H_2O$ (0.17 g, 1.00 mmol). The resulting dark green slurry was stirred for 40 min, filtered and the filtrate was layered with Et_2O/*n*-hexane (1:1 v/v, 20 mL). After 3 days, X-ray quality, green prismatic crystals of **1** were collected by filtration, washed with CH_2Cl_2 (2 × 2 mL) and Et_2O (2 × 3 mL), and dried in air. Yield: 80%. *Anal.* Calc. for $C_{34}H_{20}Cu_2F_{12}N_4O_6$: C, 43.65; H, 2.15; N, 5.99. Found: C, 43.51; H, 2.03; N, 6.04%. IR data (KBr pellet, cm^{-1}): 1652s, 1598m, 1548w, 1524m, 1488m, 1470m, 1442w, 1256s, 1218s, 1138vs, 1088w, 1030w, 984w, 792m, 748m, 712m, 666m, 582 m, 454m.

2.2.2. $[Cu_2(hfac)_2\{(py)pko\}_2]$ (**2**) and $[CuCl\{(py)pko\}\{(py)pkoH\}]{\cdot}CH_2Cl_2$ (**3**$\cdot CH_2Cl_2$) in a mixture

To a stirred, colorless solution of (py)pkoH (0.20 g, 1.00 mmol) and Na(hfac) (0.23 g, 1.00 mmol) in CH_2Cl_2 (30 mL) was added solid $CuCl_2{\cdot}2H_2O$ (0.17 g, 1.00 mmol). The resulting dark green slurry was stirred for 40 min, filtered and the filtrate was left undisturbed in a closed flask at ambient temperature. After 5 days, X-ray quality, green plate-like crystals of **2** *and* green rod-like crystals of **3**$\cdot CH_2Cl_2$ were collected by filtration, washed with CH_2Cl_2 (2 × 2 mL) and Et_2O (2 × 3 mL), and dried in air. The two products were separated manually and individually identified as complexes **2** and **3**$\cdot CH_2Cl_2$, respectively, by single-crystal, X-ray crystallography. Typical yields were ~10% (**2**) and ~40% (**3**).

2.2.3. $[Cu_2(hfac)_2\{(py)pko\}_2]$ (**2**)

To a stirred, colorless solution of (py)pkoH (0.20 g, 1.00 mmol) and Na(hfac) (0.46 g, 2.00 mmol) in CH_2Cl_2 (30 mL) was added solid $CuCl_2{\cdot}2H_2O$ (0.17 g, 1.00 mmol). The resulting dark green slurry was stirred for 40 min, filtered and the filtrate was layered with Et_2O/*n*-hexane (1:1 v/v, 30 mL). After 4 days, X-ray quality, green plate-like crystals of **2** were collected by filtration, washed with CH_2Cl_2 (2 × 2 mL) and Et_2O (2 × 3 mL), and dried in air. Yield: 60%. *Anal.* Calc. for $C_{32}H_{18}Cu_2F_{12}N_6O_6$: C, 40.99; H, 1.94; N, 8.96. Found: C, 41.12; H, 2.06; N, 8.89%. IR data (KBr pellet, cm^{-1}): 1650s, 1600m, 1574w, 1554m, 1528s, 1484s, 1440m, 1342m, 1258s, 1198vs, 1140s, 1086m, 1062w, 1030m, 1018m, 952m, 904w, 798s, 760m, 694w, 668s, 586m, 528w, 478w.

2.2.4. $[CuCl\{(py)pko\}\{(py)pkoH\}]{\cdot}CH_2Cl_2$ (**3**$\cdot CH_2Cl_2$)

To a stirred, colorless solution of (py)pkoH (0.40 g, 2.00 mmol) and NEt_3 (0.14 mL, 1.00 mmol) in CH_2Cl_2 (30 mL) was added $CuCl_2{\cdot}2H_2O$ (0.17 g, 1.00 mmol). The resulting dark green solution was stirred for 30 min, filtered and layered with Et_2O/*n*-hexane (1:1 v/v, 60 mL). After 4–5 days, X-ray quality, green rod-like crystals of **3**$\cdot CH_2Cl_2$ were collected by filtration, washed with CH_2Cl_2 (2 × 2 mL) and Et_2O (2 × 3 mL), and dried in air. Yield: 70%. The dried sample analyzed as CH_2Cl_2-free. *Anal.* Calc. for $C_{22}H_{17}CuClN_6O_2$: C, 53.23; H, 3.45; N, 16.93. Found: C, 53.16; H, 3.36; N, 17.04%. IR data (KBr pellet, cm^{-1}): 3448mb, 3046m, 1586s, 1566w, 1528w, 1470vs, 1438m, 1306w, 1286w, 1218m, 1152sh, 1136m, 1108m, 1099sh, 1054w, 1020m, 994m, 980w, 834sh, 800m, 786m, 748m, 728s, 700s, 650m, 608m, 534w, 470w.

2.3. Single-crystal X-ray crystallography

Crystallographic data and structure refinement details for the three complexes are summarized in Table 1. Selected crystals of **2** (0.50 × 0.22 × 0.06 mm) and **3**$\cdot CH_2Cl_2$ (0.70 × 0.30 × 0.20 mm) were mounted in air, whereas a selected crystal of **1** (0.45 × 0.25 × 0.20 mm) was mounted in capillary filled with drops of mother liquor. Crystallographic data for complex **1** were collected on a $P2_1$ Nicolet diffractometer upgraded by Crystal Logic using graphite-monochromated Cu radiation. Diffraction measurements for complexes **2** and **3**$\cdot CH_2Cl_2$ were made on a Crystal Logic Dual Goniometer diffractometer using graphite-monochromated Mo radiation. Unit cell dimensions were determined and refined by using the angular settings of 25 automatically centered reflec-

Table 1
Crystallographic data for complexes **1**, **2** and **3**·CH_2Cl_2.

Parameter	**1**	**2**	**3**·CH_2Cl_2
Formula	$C_{34}H_{20}Cu_2F_{12}N_4O_6$	$C_{32}H_{18}Cu_2F_{12}N_6O_6$	$C_{23}H_{19}CuCl_3N_6O_2$
Formula weight	935.62	937.60	581.33
Crystal system	triclinic	monoclinic	triclinic
Space group	$P\bar{1}$	$P2_1/a$	$P\bar{1}$
α (Å)	9.921(4)	8.628(5)	8.872(4)
b (Å)	13.203(6)	15.122(9)	11.523(6)
c (Å)	7.755(3)	13.833(8)	12.878(7)
α (°)	83.78(2)	90	110.71(2)
β (°)	70.25(2)	100.70(2)	94.82(2)
γ (°)	69.82(2)	90	91.33(2)
V (Å^3)	897.3(6)	1773.4(18)	1225.1(11)
Z	1	2	2
ρ_{calc} (g cm^{-3})	1.731	1.756	1.576
Radiation, λ (Å)	Cu Kα, 1.54180	Mo Kα, 0.71073	Mo Kα, 0.71073
Temperature (K)	298	298	298
μ (mm^{-1})	2.508	1.316	1.253
Data collected/unique (R_{int})	2445/2318 (0.0431)	3263/3130 (0.0424)	4835/4321 (0.0105)
Data with $I > 2\sigma(I)$	2192	2360	3954
R_1 ($I > 2\sigma(I)$)[a]	0.0498	0.0617	0.0361
wR_2 ($I > 2\sigma(I)$)[b]	0.1351	0.1524	0.0994

[a] $R_1 = \sum(|F_o| - |F_c|)/\sum(|F_o|)$.
[b] $wR_2 = \{\sum[w(F_o^2 - (F_c^2)^2]/\sum[w((F_o^2)^2]\}^{1/2}$.

tions in the range 22° < 2θ < 54° (for **1**) and 11° < 2θ < 22° (for **2** and **3**·CH_2Cl_2). Intensity data were recorded using a θ–2θ scan to a maximum 2θ value of 118° (for **1**) and 50° (for **2** and **3**·CH_2Cl_2). Note that the crystals of **1**, despite their sufficient size, had poor diffraction ability and the data were therefore collected in increasing 2θ shells; the data collection was terminated when almost half of the collected shell data were unobserved. Three standard reflections monitored every 97 reflections showed less than 3% variation and no decay. Lorentz, polarization corrections were applied using Crystal Logic software. All three structures were solved by direct methods using SHELXS-97 [14a] and refined on F^2 by full-matrix least-squares techniques with SHELXL-97 [14b]. All H atoms were located by Fourier difference maps and refined isotropically. All non-H atoms were refined anisotropically. For complex **1**, the fluorine atoms of the hexafluoroacetylacetonato (hfac$^-$) ligands were found disordered and refined over two positions with occupation factors fixed at 0.50. As a result of the disordered positions, the fluorine atoms present large thermal motion.

3. Results and discussion

3.1. Brief synthetic comments and IR spectra

The 1:1:2 reaction between $CuCl_2 \cdot 2H_2O$, ppkoH and Na(hfac) in CH_2Cl_2 gave a slurry, which was filtered to remove insoluble NaCl. Crystallization of the dark green solution gave green prisms of **1** in high yield (~80%). The same complex is isolated from the 1:1 Cu(hfac)$_2$/ppkoH in CH_2Cl_2 (this procedure is not reported in the experimental section); however, the yield was lower (~50%).

We then decided to seek the (py)pko$^-$ version of complex **1**. Our main goal was to determine whether the (py)pko$^-$ product would have a similar molecular structure. Due to the presence of an extra donor atom in the ligand, we might obtain more than one products from the use of the hfac$^-$/(py)pkoH ligand combination ("blend") in Cu^{II} chemistry; one dinuclear with a structure similar to that of **1** and possibly a high-nuclearity cluster in which the (py)pko$^-$ ligand would be tetradentate. Our expectations proved to be both correct and incorrect; we did obtain two products, but the second compound is a hfac$^-$-free, mononuclear complex. Green plate-like crystals of **2** and green rod-like crystals of **3**·CH_2Cl_2, in an approximate 1:1 visual ratio, were simultaneously isolated from the 1:1:1 $CuCl_2 \cdot 2H_2O$/(py)pkoH/Na(hfac) reaction mixture in CH_2Cl_2; both types of crystals were of X-ray quality.

With the identities of **2** and **3** established by crystallographic studies, a conventional high-yield synthesis of **3** was easily established by avoiding the presence of hfac$^-$ in the reaction. The reaction of $CuCl_2 \cdot 2H_2O$ with (py)pkoH and NEt_3 in an 1:2:1 ratio in CH_2Cl_2 gave a dark green solution and the subsequent isolation of **3** (~65%). Further increase of the amount of base should be avoided. Ratios of (py)pkoH to NEt_3 between 1:0.5 and 1:1 lead to a mixture of green crystals of **3** and green-black crystals of the known [13a,c] complex [Cu$_2${(py)pko}$_4$], while ratios between 1:1 and 1:1.5 give exclusively the latter compound.

In order to prepare exclusively pure **2** in a rational manner, we had to deprotonate all the available quantity of (py)pkoH in solution; we thus increased the hfac$^-$:(py)pkoH ratio in the 1:1 $CuCl_2 \cdot 2H_2O$/(py)pkoH reaction mixture. The 1:1:2 reaction between $CuCl_2 \cdot 2H_2O$, (py)pkoH and Na(hfac) in CH_2Cl_2 gave a slurry, which was filtered to remove insoluble NaCl. Layering of the resultant dark green solution with Et_2O/n-hexane gave **2** in good yield (~60%). As expected **3** is easily transformed into **2** by treatment with one equivalent of Na(hfac).

The presence of a neutral oxime group in **3** is manifested by a medium intensity, broad band at ~3450 cm^{-1} assigned to ν(OH); its broadness and relatively low wavenumber are both indicative of a hydrogen bonding [11c]. The in-plane deformation band of the 2-pyridyl ring of free ppkoH at 622 cm^{-1} shifts upwards in **1** (666 cm^{-1}), confirming the involvement of the ring N-atom in coordination [15]. The corresponding band in the spectrum of free (py)pkoH appears at 600 cm^{-1}. The appearance of two bands in this region in the spectra of **2** and **3**, one at approximately the same wavenumber (586 cm^{-1} in **2**, 608 cm^{-1} in **3**) and the other at a higher wavenumber (668 cm^{-1} in **2**, 650 cm^{-1} in **3**), reflects the presence of both coordinated and uncoordinated 2-pyridyl groups (vide infra) in the two complexes. The medium band at 1094 cm^{-1} for free ppkoH is assigned to the $\nu(NO)_{oxime}$ mode [15], which increases to 1138 cm^{-1} in **1**. This shift to higher wavenumbers has been discussed [11c] and is in accord with thee fact that upon deprotonation and oximate O-coordination, there is a higher contribution of N=O to the electronic structure of the oximate group; consequently, the ν(NO) vibration shifts to a higher wavenumber relative to that for ppkoH. The ν(NO) vibration of the coordinated oximato group appears at 1140 cm^{-1} in **2** [11c]. The 1108 cm^{-1}

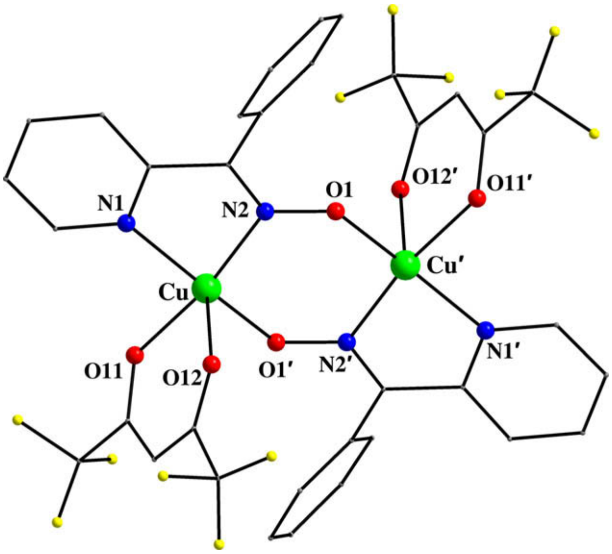

Fig. 1. Partially labeled PovRay representation of complex **1**, with H atoms omitted for clarity. Primes are used for symmetry-related atoms. Color scheme: Cu^{II}, green; O, red; N, blue; F, yellow; C, gray. (For interpretation of the references to color in this figure legend, the reader is referred to the web version of this article.)

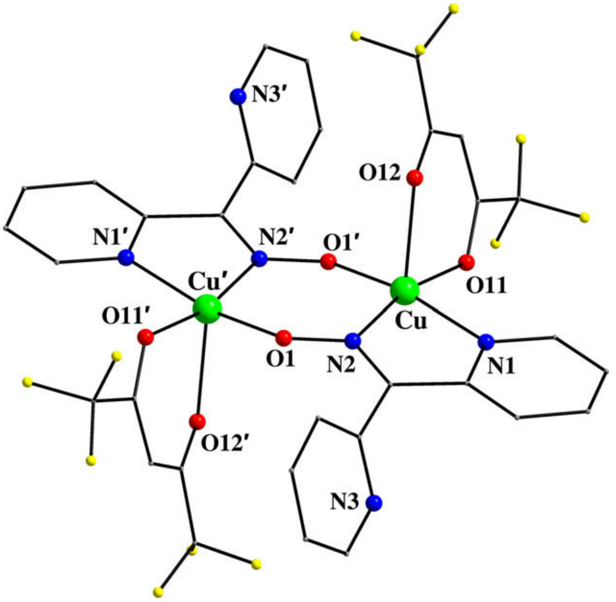

Fig. 2. Partially labeled PovRay representation of complex **2**. H atoms have been omitted for clarity. Primes are used for symmetry-related atoms. Color scheme: Cu^{II}, green; O, red; N, blue; F, yellow; C, gray. (For interpretation of the references to color in this figure legend, the reader is referred to the web version of this article.)

band in the spectrum of **3** is a serious candidate for the $\nu(\mathrm{NO}\cdots\mathrm{H})$ vibration.

The strong band at 1652 and 1650 cm^{-1} in the spectra of **1** and **2**, respectively, is assigned to the $\nu(\mathrm{C}\cdots\mathrm{O})$ mode of the *O,O′*-chelating hfac$^-$ ligand [16,17]. This band appears at almost the same wavenumber (1644 cm^{-1}) for complex [Cu(hfac)$_2$], in which the hfac$^-$ ion is chelated to the metal [16].

3.2. Description of structures

The molecular structures of complexes **1**, **2** and **3** are depicted in Figs. 1, 2 and 4, respectively. Selected interatomic distances and angles are listed in Tables 2–4.

Complex **1** crystallizes in the triclinic space group $P\bar{1}$. Its structure consists of isolated dinuclear [Cu$_2$(hfac)$_2$(ppko)$_2$] molecules (Fig. 1). There is a crystallographic inversion center at the mid-point of the $Cu^{II}\ldots Cu^{II}$ axis. The Cu^{II} atoms are doubly bridged by the diatomic oximate groups of two $\eta^1{:}\eta^1{:}\eta^1{:}\mu_2$ ppko$^-$ ligands (Scheme 2); each ligand chelates one Cu^{II} atom forming a five-membered CuNCCN chelating ring, while its oximate oxygen atom is terminally bound to the other metal center. The bridging CuN(2)O(1)Cu′ unit is not planar; the torsion angle is 23.2°. The deviations of atoms Cu, O(1), N(2) and Cu′ from the CuN(2)O(1)Cu′ best mean plane are 0.035, 0.100 Å above, and 0.099, 0.034 Å below the plane, respectively. A bidentate chelating (η^2) hfac$^-$ ligand (Scheme 2) completes five-coordination at each metal. Analysis of the shape-determining bond angles using the approach of Reedijk and co-workers [18] yields a value for the trigonality index, τ, of 0.11 for the metal ions ($\tau = 0$ and 1 for perfect square pyramidal and trigonal bipyramidal geometries, respectively). Thus, the geometry about each Cu^{II} center can be described as slightly distorted square pyramidal (sp), with the apical position of Cu occupied by an oxygen atom [O(12)] of a chelating hfac$^-$ ligand. One 2-pyridyl [N(1)] and an oximate [N(2)] nitrogen atom arising from the same bridging ppko$^-$ ligand, as well as the oximate oxygen atom [O(1′)] from the other ppko$^-$ ligand and the remaining oxygen atom [O(11)] of a hfac$^-$ group form the basal plane for Cu. As expected, the Cu–O(12) bond distance is the longest. Cu lies 0.147 Å out of the basal plane towards O(12). The $\mathrm{Cu}\cdots\mathrm{Cu}'$ distance is 3.699(1) Å. There are no significant intermolecular interactions, either hydrogen bonds or π–π stacking interactions.

Complex **2** crystallizes in the monoclinic space group $P2_1/a$. Its structure (Fig. 2) is very similar to that of **1**, with the only difference being the nature of the bridging oximate ligands, i.e., the two Cu^{II} atoms in centrosymmetric complex **2** are doubly bridged by the diatomic oximate groups of two $\eta^1{:}\eta^1{:}\eta^1{:}\mu_2$ (py)pko$^-$ groups (Scheme 2) instead of two $\eta^1{:}\eta^1{:}\eta^1{:}\mu_2$ ppko$^-$ groups that are present in **1**. The bridging CuN(2)O(1)Cu′ unit is again not planar with the torsion angle being 20.3°, slightly less than the corresponding value for complex **1**. The deviations of atoms Cu, O(1), N(2) and Cu′ from the CuN(2)O(1)Cu′ best mean plane are 0.029, 0.085 Å above, and 0.083, 0.030 Å below the plane, respectively. A bidentate chelating (η^2) hfac$^-$ ligand completes five-coordination at each metal. The metal coordination geometry is described as almost perfect square pyramidal ($\tau = 0.03$ [18]), with the apical position of Cu occupied by an oxygen atom [O(12)] of the chelating hfac$^-$ ligand. Cu lies 0.220 Å out of the basal plane towards O(12), while the $\mathrm{Cu}\cdots\mathrm{Cu}'$ distance is 3.772(2) Å, slightly longer than that in **1**.

It is of interest to note that the crystal structure of **2** is further stabilized by four symmetry-equivalent, intermolecular $\mathrm{F}\cdots\mathrm{F}$ Van der Waals contacts [$\mathrm{F(2)}\cdots\mathrm{F(5)} = 2.92(2)$ Å] which serve to link neighboring Cu$_2$ dimers into one-dimensional double chains along the *a* axis (Fig. 3, top). These interactions create vacant (from cocrystallized solvent molecules) channels (Fig. 3, bottom).

Complex **2** is structurally similar to compound [Cu$_2${(py)pko}$_4$]·2H$_2$O [13a,c]; in the latter the capping terminal ligands are provided by two η^2 (py)pko$^-$ groups (instead of the two hfac$^-$ ligands that are present in the former).

Complex **3**·CH$_2$Cl$_2$ crystallizes in the triclinic space group $P\bar{1}$. Its structure consists of well-separated [CuCl{(py)pko}{(py)pkoH}] molecules (Fig. 4) and solvate CH$_2$Cl$_2$ molecules in an 1:1 ratio; the latter will not be further discussed. The Cu^{II} center is coordinated by a monodentate Cl$^-$ group and two *N,N′*-bidentate chelating (η^2) (py)pko$^-$ and (py)pkoH ligands (Scheme 2). There is a hydrogen atom [HO(11)] located at practically the middle of the oximate oxygen atoms' distance [O(1)–HO(11) 1.20(5)/O(11)–HO(11) 1.26(5) Å]; this prevents any clear assignment on the exact position of HO(11) and consequently a precise attribution of the

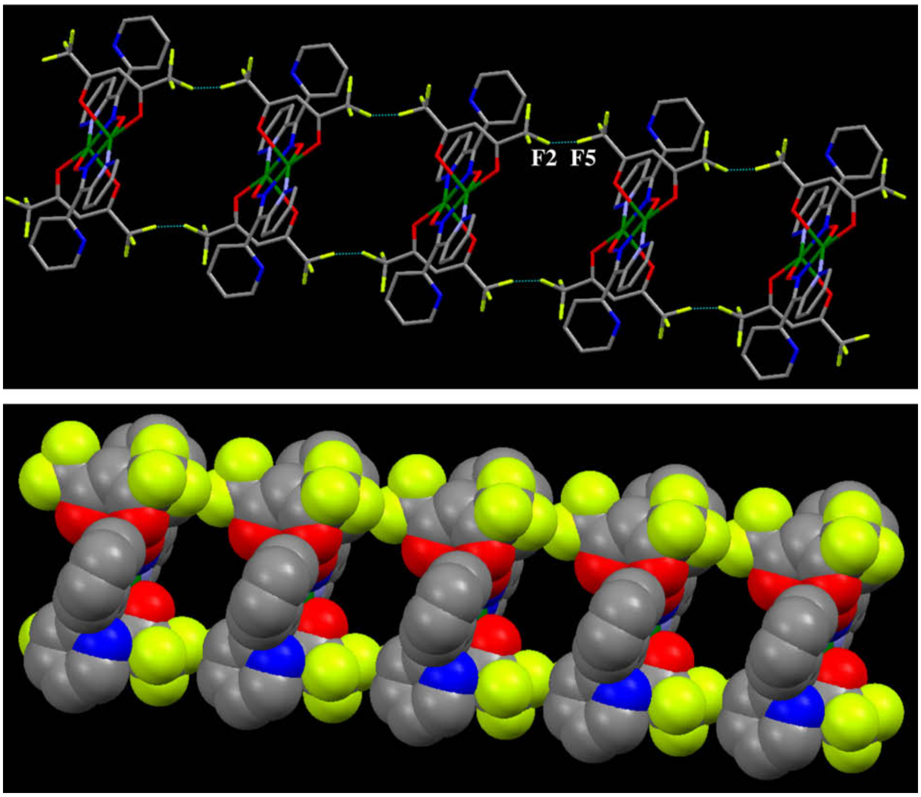

Fig. 3. Top: A partially labeled section of the 1D double chains of **1** illustrating the inter-dimer F···F linkages through the hfac$^-$ groups along the *a* axis. Bottom: Space-filling representation viewed along the *a* axis, emphasizing the large channels that are present in the crystal structure. Color scheme: Cu^{II}, green; O, red; N, blue; F, yellow; C, gray. (For interpretation of the references to color in this figure legend, the reader is referred to the web version of this article.)

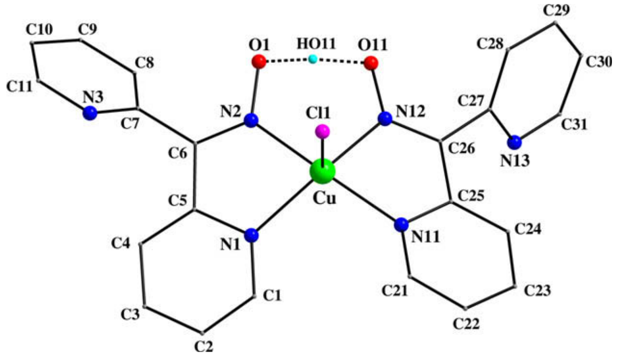

Fig. 4. Labelled PovRay representation of **3**, with some H atoms omitted for clarity. The dashed lines are H-bonds. Color scheme: Cu^{II}, green; O, red; N, blue; Cl, purple; C, gray; H, sky blue. (For interpretation of the references to color in this figure legend, the reader is referred to the web version of this article.)

Table 2
Selected interatomic distances (Å) and angles (°) for complex **1**.[a]

Cu–O(1′)	1.914(2)	Cu–N(1)	1.993(3)
Cu–O(11)	1.993(2)	Cu–N(2)	1.978(3)
Cu–O(12)	2.230(3)	Cu···Cu′	3.699(1)
O(1′)–Cu–O(11)	84.5(1)	O(11)–Cu–N(1)	90.0(1)
O(1′)–Cu–O(12)	93.0(1)	O(11)–Cu–N(2)	171.2(1)
O(1′)–Cu–N(1)	164.7(1)	O(12)–Cu–N(1)	101.0(1)
O(1′)–Cu–N(2)	103.4(1)	O(12)–Cu–N(2)	95.5(1)
O(11)–Cu–O(12)	87.9(1)	N(1)–Cu–N(2)	81.4(1)

[a] Primed atoms are related to the unprimed ones by the symmetry operation $-x$, $2-y$, $-z$.

Table 3
Selected interatomic distances (Å) and angles (°) for complex **2**.[a]

Cu–O(1′)	1.908(4)	Cu–N(1)	1.990(5)
Cu–O(11)	1.984(4)	Cu–N(2)	1.974(5)
Cu–O(12)	2.243(5)	Cu···Cu′	3.772(2)
O(1′)–Cu–O(11)	84.8(2)	O(11)–Cu–N(1)	90.0(2)
O(1′)–Cu–O(12)	88.9(2)	O(11)–Cu–N(2)	166.6(2)
O(1′)–Cu–N(1)	164.8(2)	O(12)–Cu–N(1)	105.1(2)
O(1′)–Cu–N(2)	101.3(2)	O(12)–Cu–N(2)	105.2(2)
O(11)–Cu–O(12)	86.6(2)	N(1)–Cu–N(2)	81.1(2)

[a] Primed atoms are related to the unprimed ones by the symmetry operation $-x$, $2-y$, $1-z$.

Table 4
Selected bond lengths (Å) and angles (°) for complex $\mathbf{3}\cdot CH_2Cl_2$.

Cu–N(1)	2.052(2)	Cu–N(12)	2.008(2)
Cu–N(2)	1.991(2)	Cu–Cl(1)	2.407(1)
Cu–N(11)	2.045(2)		
N(1)–Cu–N(2)	78.63(9)	N(11)–Cu–N(12)	78.94(9)
N(1)–Cu–N(11)	103.52(9)	Cl(1)–Cu–N(1)	102.30(7)
N(1)–Cu–N(12)	151.60(9)	Cl(1)–Cu–N(2)	96.96(8)
N(2)–Cu–N(11)	165.29(9)	Cl(1)–Cu–N(11)	96.77(7)
N(2)–Cu–N(12)	92.29(9)	Cl(1)–Cu–N(12)	105.50(7)

negative charge on one of the two ligands. Undoubtedly, this is a very strong intramolecular H-bond between the two oximate oxygen atoms, with its existence rationalizing the high thermodynamic stability of **3**; the dimensions are: O(1)···O(11) 2.442(3) Å and O(1)–HO(11)···O(11) 169.1(5)°. Alternatively, the two di-2-pyridyl ketone oximate/oxime groups can be considered as one tetradentate N_4-chelating {(py)pko···H···(py)pko} ligand. The $\succcurlyeq$CN–O···H···O–NC$\preccurlyeq$ motif is a valuable synthon in crystal engineering [19].

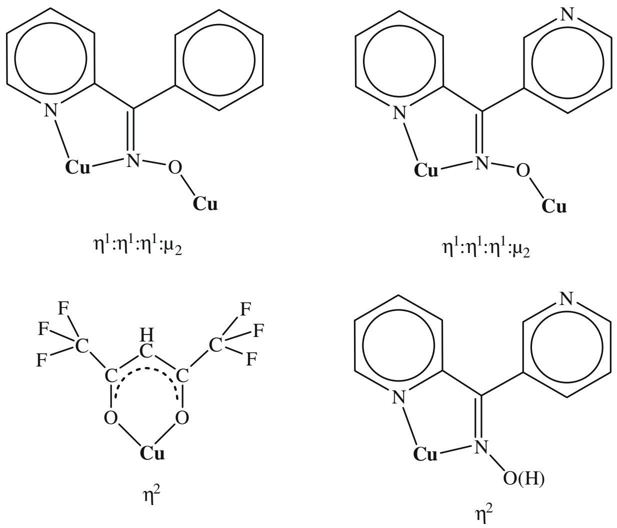

Scheme 2. The crystallographically established coordination modes of the ligands discussed in the text.

The donor atoms are the oxime/oximate nitrogens [N(2), N(12)] and two pyridyl nitrogens [N(1), N(11)], each from a different ligand. One terminal chloro ligand [Cl(1)] completes five-coordination at the metal center. The Cu–N bond lengths are normal for this class of compound [12,13], whereas the Cu–Cl(1) distance [2.407(1)Å] indicates a rather weak, but not abnormally weak [20], copper(II)–chloro bond. The metal coordination geometry is well described as square pyramidal with the chloro ligand occupying the apical position. Analysis of the shape-determining angles [18] yields a value for the trigonality index, τ, of 0.23, indicating that the geometry about copper is significantly distorted. The four nitrogen atoms N(1), N(2), N(11) and N(12) define the basal plane, deviating from this plane by an average of 0.12 Å [maximum deviation by N(2) and N(12), 0.131 Å]; the metal ion lies 0.363 Å out of the best, least-squares basal plane, towards Cl(1).

The mononuclear molecules seem to be stabilized in the crystal by a strong intermolecular π–π stacking interaction between (py)pko$^-$/(py)pkoH ligands of adjacent molecules. The interaction involves the uncoordinated 2-pyridyl rings that possess N(3) and N(3′) (Fig. 5); the intercentroid distance ($C_g \cdots C_g'$) is 3.275 Å and the rings are perfectly planar to each other. Complexes **1**–**3** join a very small family of structurally characterized copper(II) compounds with the neutral and anionic derivatives of ppkoH and (py)pkoH [2c,12,13,21].

3.3. Magnetochemistry

Magnetostructural studies on polynuclear metal complexes are of continuing interest for coordination chemists since they can provide the understanding of fundamental factors governing their magnetic properties. The bridging diatomic =N–O$^-$ group is known to be very efficient in mediating a medium-to-strong antiferromagnetic interaction, which is provided by an orbital exchange pathway of σ symmetry, giving values of the coupling constants, J_{ij}, typically greater than $-500\ \mathrm{cm}^{-1}$. Thus, for instance, Cu^{II} complexes with double oximato bridges usually exhibit complete or nearly complete spin coupling even at room temperature [22].

Variable-temperature dc magnetic susceptibility data in an 1.0 T field and in the 2.0–300 K range were collected on a powdered microcrystalline sample of the representative dinuclear compound **1** restrained in eicosane to prevent torquing. The obtained data are plotted as $\chi_M T$ versus T in Fig. 6. The $\chi_M T$ value at 300 K is only 0.082 cm^3 mol^{-1} K. This value is much lower than that expected for a molecule comprising two non-interacting Cu^{II} ions (0.75 cm^3 mol^{-1} K with $g = 2$). The $\chi_M T$ product rapidly decreases with decreasing temperature, reaching a constant value very close to 0 cm^3 mol^{-1} K at ~100 K. This behavior is indicative of very strong antiferromagnetic interactions between the metal centers with the low temperature value suggesting a well-isolated singlet ground-state spin ($S = 0$). Thus, complex **1** is essentially diamagnetic even at room temperature, in a way that at the whole temperature range (2.0–300 K) the $S = 0$ state is mainly populated. In accordance with this, the polycrystalline EPR spectrum of the complex shows no signal in this temperature range. On the other hand, the molar magnetic susceptibility χ_M shows a continuous decrease upon cooling down to a broad minimum centered at ~130 K, but below this temperature it rapidly increases due to the presence of a small amount of paramagnetic, possibly monomeric, impurity. The maximum of χ_M should be located at a temperature much larger than 300 K in agreement with the very strong antiferromagnetic interaction suggested by the $\chi_M T$ data.

A fit of the experimental data of **1** to the expression derived from the simplified spin Hamiltonian, $H = -J(S_1 \cdot S_2)$, and introducing a ρ term to evaluate the monomeric paramagnetic impurity, gives the parameters $J = -720(10)\ \mathrm{cm}^{-1}$, $g = 2.15(6)$ and $\rho = 0.13(5)\%$, which lead to a quasi perfectly isolated $S = 0$ ground state with the $S = 1$ excited state (triplet state) being 1440 cm^{-1} above the ground state. This magnetic behavior is not unexpected in view of

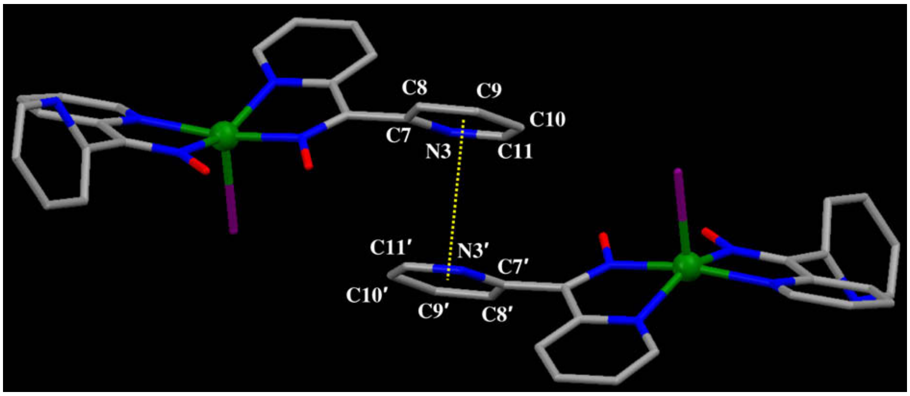

Fig. 5. A partially labeled representation of the intermolecular π–π stacking interaction (yellow dashed line) found in **3**, which serves to link adjacent monomers in the crystal. Color scheme: Cu^{II}, green; O, red; N, blue; Cl, purple; C, gray. (For interpretation of the references to color in this figure legend, the reader is referred to the web version of this article.)

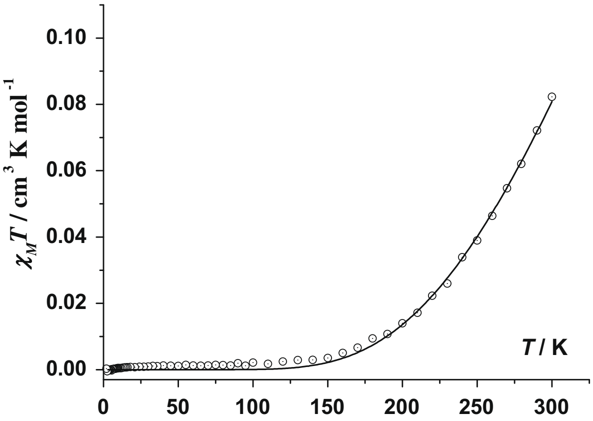

Fig. 6. Plot of $\chi_M T$ vs. T for **1** in a 10 kG field. The solid lines are the best fit of the experimental data; see the text for the fit parameters.

the remarkable ability of the oximato bridges to mediate strong antiferromagnetic exchange interactions between paramagnetic centers, either in *syn*, *anti*, or *O*-monoatomic coordination [1a,22]. Extended-Huckel MO calculations previously reported by some of us [22h] and others [22f] on the Cu–(R=N–O)$_2$–Cu core (R = various substituted groups) have indicated that planar Cu–(R=N–O)$_2$–Cu "rings" favor the strongest magnetic coupling, but other factors such as the electronic properties of the R-substituted oximato groups and/or the ligands that complete the coordination sphere of the Cu^{II} ions (i.e., hfac$^-$ in **1** and **2**) play an important role modulating the magnitude of the coupling [22h]. Complex **1** exhibits a very strong antiferromagnetic coupling ($J = -720$ cm^{-1}) typical for the members of the family of doubly *N*,*O* oximato-bridged Cu^{II}_2 complexes [22f,22h]. The coupling interaction is almost the same with that observed in complex $[Cu_2(Hboa)_2(H_2O)_2](ClO_4)_2$, where Hboa$^-$ is the monoanion of biacetyl oxime azine [23]. Of particular interest is complex $[LCu^{II}\{(py)C(H)NO\}_2Cu^{II}I](ClO_4)$, where L = 1,4,7-trimethyl-1,4,7-triazacyclononane and (py)C(H)NO$^-$ the 2-pyridylaldoximate(-1) ligand, in which the Cu^{II} centers are very strongly antiferromagnetically coupled, the singlet–triplet splitting being greater than 1000 cm^{-1}. It should be mentioned at this point that the structurally similar complex $[Cu_2\{(py)pko\}_4]\cdot 2H_2O$ [13c] is also diamagnetic at room temperature; however, an estimation of the coupling constant was not provided.

4. Conclusions

The present work extends the body of results that emphasize the ability of 2-pyridyl oximes to form interesting structural types in Cu^{II} coordination chemistry when they are combined with suitable ancillary ligands, such as carboxylates [12] or non-carboxylates [13]. The employment of the Cu/hfac$^-$/(py)C(R)NOH (R = ph, py) reaction system has provided access to two new members of the growing family of doubly, *N*,*O* oximato-bridged dinuclear complexes and a mononuclear, hfac$^-$-free compound $[CuCl\{(py)pko\}\{(py)pkoH\}]$ (**3**). The representative dinuclear complex **1** has been found to possess an isolated $S = 0$ spin ground state due to the very strong antiferromagnetic coupling between the two Cu^{II} centers through the double =N–O$^-$ bridges. This coupling gives a massive value for the coupling constant J of -720 cm^{-1}. In order to gain more insight into this important subject, i.e., the in-depth understanding of the exact structural parameters that influence the sign and strength of the magnitude of the coupling in the Cu–(R=N–O)$_2$–Cu type of complexes, more examples of such compounds are needed, preferably closely related ones displaying variation over only one of the structural parameters. For example, we are currently exploring the reactions of 2-pyridyl oximes with copper(II) acetylacetonate in order to test the differences in the magnetic coupling induced by various β-diketonate ligands. Work also is in progress in our groups to synthesize high-nuclearity copper(II)/β-diketonate/2-pyridyl oximate clusters.

Supplementary data

CCDC 730888, 730889 and 730890 contain the supplementary crystallographic data for **1**, **2** and **3**. These data can be obtained free of charge via http://www.ccdc.cam.ac.uk/conts/retrieving.html, or from the Cambridge Crystallographic Data Centre, 12 Union Road, Cambridge CB2 1EZ, UK; fax: (+44) 1223-336-033; or e-mail: deposit@ccdc.cam.ac.uk.

Acknowledgements

This work was supported by EPEAEK II (Program PYTHAGORAS I, Grant b.365.037 to S.P.P.) and MEC (Grant CTQ2006-01759 to A.E.). We thank K.A. Kounavi for experimental assistance.

References

[1] (a) For an excellent review, see P. Chaudhuri, Coord. Chem. Rev. 243 (2003) 143;
(b) A.J.L. Pombeiro, V. Yu Kukushkin, in: J.A. McCleverty, T.J. Meyer (Eds.), Comprehensive Coordination Chemistry II, vol. 1, Elsevier, Amsterdam, 2004, p. 631.

[2] (a) R.J. Butcher, C.J. O'Connor, E. Sinn, Inorg. Chem. 20 (1981) 537;
(b) C.J. Milios, C.P. Raptopoulou, A. Terzis, F. Lloret, R. Vicente, S.P. Perlepes, A. Escuer, Angew. Chem., Int. Ed. 43 (2004) 210;
(c) For a comprehensive review, see:C.J. Milios, Th.C. Stamatatos, S.P. Perlepes, Polyhedron 25 (2006) 134 (Polyhedron Report);
(d) For an excellent review, see: C.J. Milios, S. Piligkos, E.K. Brechin, Dalton Trans. (2008) 1809 (Dalton Perspective);
(e) Th.C. Stamatatos, C. Papatriantafyllopoulou, E. Katsoulakou, C.P. Raptopoulou, S.P. Perlepes, Polyhedron 26 (2007) 1830.

[3] (a) P. Chaudhuri, M. Winter, F. Birkelbach, P. Fleischhauer, W. Haase, U. Flörke, H.-J. Haupt, Inorg. Chem. 30 (1991) 4291;
(b) S. Ross, T. Weyhermüller, E. Bill, K. Wieghardt, P. Chaudhuri, Inorg. Chem. 40 (2001) 6656;
(c) C. Lampropoulos, Th.C. Stamatatos, K.A. Abboud, G. Christou, Inorg. Chem. 48 (2009) 429;
(d) S. Khanra, T. Weyhermüller, P. Chaudhuri, Dalton Trans. (2007) 4675.

[4] For example, see: R. Clérac, H. Miyasaka, M. Yamashita, C. Coulon, J. Am. Chem. Soc. 124 (2002) 12837.

[5] F. Mori, T. Nyui, T. Ishida, T. Nogami, K.-Y. Choi, H. Nojiri, J. Am. Chem. Soc. 128 (2006) 1440.

[6] For an excellent review, see: H. Miyasaka, R. Clérac, Bull. Chem. Soc. Japan 78 (2005) 1725.

[7] (a) C.J. Milios, P. Kyritsis, C.P. Raptopoulou, A. Terzis, R. Vicente, A. Escuer, S.P. Perlepes, Dalton Trans. (2005) 501;
(b) Th.C. Stamatatos, K.V. Pringouri, C.P. Raptopoulou, R. Vicente, V. Psycharis, A. Escuer, S.P. Perlepes, Inorg. Chem. Commun. 9 (2006) 1178;
(c) K.V. Pringouri, C.P. Raptopoulou, A. Escuer, Th.C. Stamatatos, Inorg. Chim. Acta 360 (2007) 69.

[8] (a) C.J. Milios, C.P. Raptopoulou, A. Terzis, R. Vicente, A. Escuer, S.P. Perlepes, Inorg. Chem. Commun. 6 (2003) 1056;
(b) C.J. Milios, E. Kefalloniti, C.P. Raptopoulou, A. Terzis, R. Vicente, N. Lalioti, A. Escuer, S.P. Perlepes, Chem. Commun. (2003) 819;
(c) C.J. Milios, E. Kefalloniti, C.P. Raptopoulou, A. Terzis, A. Escuer, R. Vicente, S.P. Perlepes, Polyhedron 23 (2004) 83;
(d) C.J. Milios, Th.C. Stamatatos, P. Kyritsis, A. Terzis, C.P. Raptopoulou, R. Vicente, A. Escuer, S.P. Perlepes, Eur. J. Inorg. Chem. (2004) 2885;
(e) Th.C. Stamatatos, D. Foguet-Albiol, C.C. Stoumpos, C.P. Raptopoulou, A. Terzis, W. Wernsdorfer, S.P. Perlepes, G. Christou, J. Am. Chem. Soc. 127 (2005) 15380;
(f) Th.C. Stamatatos, D. Foguet-Albiol, S.-C. Lee, C.C. Stoumpos, C.P. Raptopoulou, A. Terzis, W. Wernsdorfer, S.O. Hill, S.P. Perlepes, G. Christou, J. Am. Chem. Soc. 129 (2007) 9484;
(g) C.C. Stoumpos, Th.C. Stamatatos, H. Sartzi, O. Roubeau, A.J. Tasiopoulos, V. Nastopoulos, S.J. Teat, G. Christou, S.P. Perlepes, Dalton Trans. (2009) 1004.

[9] Th.C. Stamatatos, A.K. Boudalis, Y. Sanakis, C.P. Raptopoulou, Inorg. Chem. 45 (2006) 7372.

[10] (a) Th.C. Stamatatos, S. Dionyssopoulou, G. Efthymiou, P. Kyritsis, C.P. Raptopoulou, A. Terzis, R. Vicente, A. Escuer, S.P. Perlepes, Inorg. Chem. 44 (2005) 3374;
(b) Th.C. Stamatatos, A. Bell, P. Cooper, A. Terzis, C.P. Raptopoulou, S.L. Heath, R.E.P. Winpenny, S.P. Perlepes, Inorg. Chem. Commun. 8 (2005) 533.

[11] (a) Th.C. Stamatatos, K.A. Abboud, S.P. Perlepes, G. Christou, Dalton Trans. (2007) 3861;
(b) Th.C. Stamatatos, E. Diamantopoulou, A. Tasiopoulos, V. Psycharis, R. Vicente, C.P. Raptopoulou, V. Nastopoulos, A. Escuer, S.P. Perlepes, Inorg. Chim. Acta 359 (2006) 4149;
(c) Th.C. Stamatatos, A. Escuer, K.A. Abboud, C.P. Raptopoulou, S.P. Perlepes, G. Christou, Inorg. Chem. 47 (2008) 11825;
(d) Th.C. Stamatatos, E. Diamantopoulou, C.P. Raptopoulou, V. Psycharis, A. Escuer, S.P. Perlepes, Inorg. Chem. 46 (2007) 2350.

[12] (a) Th.C. Stamatatos, J.C. Vlahopoulou, Y. Sanakis, C.P. Raptopoulou, V. Psycharis, A.K. Boudalis, S.P. Perlepes, Inorg. Chem. Commun. 9 (2006) 814;
(b) J.C. Vlahopoulou, Ph.D. Thesis, University of Patras, 2009.

[13] (a) E.O. Schlemper, J. Stunker, C. Patterson, Acta Crystallogr., Sect. C 46 (1990) 1226;
(b) T. Afrati, C. Dendrinou-Samara, C.M. Zaleski, J.W. Kampf, V.L. Pecoraro, D.P. Kessissoglou, Inorg. Chem. Commun. 8 (2005) 1173;
(c) T. Afrati, C.M. Zaleski, C. Dendrinou-Samara, G. Mezei, J.W. Kampf, V.L. Pecoraro, D.P. Kessissoglou, Dalton Trans. (2007) 2658;
(d) S.O. Sommerer, B.L. Westcott, A.J. Jircitano, K.A. Abboud, Inorg. Chim. Acta 238 (1995) 149;
(e) M.A.S. Goher, F.A. Mautner, Polyhedron 18 (1999) 3425.

[14] (a) G.M. Sheldrick, SHELXS-97, Structure Solving Program, University of Göttingén, Germany, 1997;
(b) G.M. Sheldrick, SHELXL-97, Program for the Refinement of Crystal Structures from Diffraction Data, University of Göttingén, Germany, 1997.

[15] C. Papatriantafyllopoulou, C.G. Efthymiou, C.P. Raptopoulou, A. Terzis, E. Manessi-Zoupa, S.P. Perlepes, Spectrochim. Acta, Part A (2008) 718.

[16] K. Nakamoto, Infrared and Raman Spectra of Inorganic and Coordination Compounds, fourth ed., Wiley, New York, 1986.

[17] N.A. Bailey, D.E. Fenton, M.S. Leal Gonzalez, Inorg. Chim. Acta 88 (1984) 125.

[18] A.W. Addison, T.N. Rao, J. Reedijk, J.V. Rijin, G.C. Verschoor, J. Chem. Soc., Dalton Trans. (1984) 1349.

[19] V.V. Ponomarova, K.V. Domasevitch, Cryst. Eng. 5 (2002) 137.

[20] K. Skorda, Th.C. Stamatatos, A.P. Vafiadis, A.T. Lithoxoidou, A. Terzis, S.P. Perlepes, J. Mrozinski, C.P. Raptopoulou, J.C. Plakatouras, E.G. Bakalbassis, Inorg. Chim. Acta 358 (2005) 565.

[21] T. Afrati, C. Dendrinou-Samara, C. Raptopoulou, A. Terzis, V. Tangoulis, D.P. Kessissoglou, Dalton Trans. (2007) 5156.

[22] (a) H. Okawa, M. Koikawa, S. Kida, D. Luneau, H. Oshio, J. Chem. Soc., Dalton Trans. (1990) 469;
(b) D. Luneau, H. Oshio, H. Okawa, S. Kida, J. Chem. Soc., Dalton Trans. (1990) 2283;
(c) P. Chaudhuri, M. Winter, B.P.C. Della Vedova, E. Bill, A. Trautwein, S. Gehring, P. Fleischauer, B. Nuber, J. Weiss, Inorg. Chem. 30 (1991) 2148;
(d) R. Ruiz, J. Sanz, B. Cervera, F. Lloret, M. Julve, C. Bois, J. Faus, M.C. Munoz, J. Chem. Soc., Dalton Trans. (1991) 1623;
(e) R. Ruiz, J. Sanz, F. Lloret, M. Julve, J. Faus, C. Bois, M.C. Munoz, J. Chem. Soc., Dalton Trans. (1993) 3035;
(f) R. Ruiz, F. Lloret, M. Julve, M.C. Munoz, C. Bois, Inorg. Chim. Acta 219 (1994) 179;
(g) E. Colacio, J.M. Dominguez-Vera, A. Escuer, M. Klinga, R. Kivekas, A. Romerosa, J. Chem. Soc., Dalton Trans. (1995) 343;
(h) J.M. Dominguez-Vera, E. Colacio, A. Escuer, M. Klinga, R. Kivekäs, A. Romerosa, Polyhedron 16 (1997) 281;
(i) P. Chaudhuri, M. Winter, U. Flörke, H.-J. Haupt, Inorg. Chim. Acta 232 (1995) 125.

[23] Y. Song, X.-T. Chen, C.-G. Zheng, D.-R. Zhu, X.-Z. You, L.-H. Weng, Transition Met. Chem. 26 (2001) 247.